



Entropic order

Received: 5 October 2025

Yiqiu Han¹, Xiaoyang Huang¹, Zohar Komargodski², Andrew Lucas¹✉ & Fedor K. Popov²

Accepted: 14 November 2025

Published online: 29 November 2025

Check for updates

Ordered phases of matter, such as solids, ferromagnets, superfluids, or quantum topological order, typically only exist at low temperatures. Despite this conventional wisdom, we present explicit local models in which all such phases persist to arbitrarily high temperature. This is possible since order in one degree of freedom can enable other degrees of freedom to strongly fluctuate, leading to entropic order, whereby typical high energy states are ordered. Our construction, which utilizes interacting bosons, avoids existing no-go theorems on long-range order or entanglement at high temperature. We propose a simple model for high-temperature superconductivity using these general principles.

Statistical mechanics is the theory of simple collective phenomena that arise out of many-body physical systems. The most striking phenomenon is that of a phase transition: as a parameter—which we take here to be temperature T —is tuned beyond a critical value T_c , the macroscopic phase of matter abruptly changes. For example, when solid ice is heated above $T_c = 0^\circ\text{C}$, it abruptly melts into liquid water.

Here, the low-temperature phase is more ordered than the high-temperature phase. Solid ice forms a crystal and spontaneously breaks translation and rotation symmetries: the crystalline lattice has a specific orientation, and the atoms prefer to be in specific places relative to others, over arbitrarily long length scales. In liquid water, there is no long-range order: translation and rotation symmetry are restored. Breaking these symmetries makes ice an ordered phase and water a disordered phase.

In thermodynamics, systems minimize the free energy

$$F = E - TS, \quad (1)$$

where E denotes energy, T temperature, and S entropy. If we cross a phase transition from A to B at some temperature T_c (in this paper, other external parameters, e.g., volume, are fixed), the high-temperature phase has higher entropy at $T > T_c$. This is readily seen from the laws of thermodynamics, which imply that $F = \min(F_A, F_B)$ and

$$S = -\frac{\partial F}{\partial T}. \quad (2)$$

Entropy is usually associated with disorder, so we expect the disordered phase at high T .

But sometimes, the ordered phase is at high temperature. This is because the ordered phase can have higher entropy, however unlikely it sounds. We will say that such a phase has entropic order. Experimental realizations include crystalline ordering in the Rochelle salt¹ and inverse melting^{2,3}; see also refs. 4,5. But the most famous example is the Pomeranchuk effect in ^3He : at $T < 10^{-7}\text{ K}$ (and 30 atm pressure) we find a liquid, while for $10^{-7}\text{ K} < T < 1\text{ K}$ we find a solid⁶. When the atoms lock into a crystal, atomic isospin degrees of freedom can freely fluctuate, while they cannot in the liquid. By sacrificing the translational entropy and forming a crystal, we overcompensate with extra isospin entropy. Analogous phenomena have also been found in magic-angle graphene⁷. A somewhat related mechanism at low temperatures is known as order by disorder⁸.

In all of these examples, upon sufficiently heating the system, one again finds a disordered phase. Under seemingly mild conditions, which we review in the Supplementary Material (SM), one can even prove that the high-temperature phase of any discrete lattice model must be disordered and have no quantum entanglement^{9,10}. At the same time, certain quantum field theories order at arbitrarily high temperature^{11–21} (closely related constructions using the AdS/CFT correspondence appeared in refs. 22–26, and some nonlocal theories were considered in refs. 27,28).

It is an outstanding question whether or not such an order is possible in simple lattice models. What is the physical mechanism for it? If it is possible to indeed avoid the no-go theorems^{9,10} on high-temperature order in lattice models, explicit models could enable more faithful simulations of the unconventional quantum field theories (QFTs) described above, and perhaps even lead to experimental realizations of high-temperature entropic order.

¹Department of Physics and Center for Theory of Quantum Matter, University of Colorado, Boulder, CO, USA. ²Simons Center for Geometry and Physics, SUNY, Stony Brook, NY, USA. ✉e-mail: andrew.j.lucas@colorado.edu

We will answer the above questions, presenting explicit models with order as $T \rightarrow \infty$, both in lattice models and field theory. Illustrative examples include high-temperature ferromagnets, solids, superfluids, quantum topological order, and superconductivity. There is a unifying principle behind all of our examples: interacting bosons have an unbounded number of fluctuations, which are enhanced by the existence of order in a second degree of freedom, e.g., spins. The bosonic entropy overcompensates for the reduced spin entropy due to ordering, and we find that the spins can order in most states at fixed (high) energy. This is why we adopt the terminology entropic order. We show that this mechanism underlies high- T order in the field theory models mentioned above. We emphasize the toy models for very high temperature superconductivity, which may guide a search for this long-sought phenomenon.

Let us briefly recall basic statistical mechanics, using a classical example for illustration (details of both classical and quantum models are in the SM). Consider a two-dimensional square lattice, where at every vertex v we choose to put $n_v \in \{0, 1\}$ particles. The collection of all $\mathbf{n} = \{n_v\}$ is called a microstate. In statistical mechanics, the probability of observing a particular microstate at temperature $T = 1/\beta$ is

$$P(\mathbf{n}) = \frac{e^{-\beta H(\mathbf{n})}}{Z(\beta)} \quad (3)$$

where $H(\mathbf{n})$ is the energy (Hamiltonian) of the microstate, and the partition function

$$Z(\beta) = \sum_{\mathbf{n}} e^{-\beta H(\mathbf{n})} = e^{-\beta F(\beta)} \quad (4)$$

both normalizes the probability distribution and defines the free energy F . A system is a many-body system if $H(\mathbf{n})$ can be expressed as a sum of terms, each of which only depends on a finite number of n_v , which we take here to be nearest-neighbors on the lattice.

A famous illustrative example of how phase transitions usually arise is the lattice gas²⁹

$$H = U \sum_{u \sim v} n_u n_v - \mu \sum_v n_v, \quad (5)$$

where $u \sim v$ denote nearest neighbors on the lattice. Here $n_u \in \{0, 1\}$. (This model is also equivalent to the Ising anti-ferromagnet in a constant magnetic field.) Let us consider $0 \leq \mu \leq 4U$, where at low temperatures, the repulsion dominates over the chemical potential. Then the ground states are a checkerboard, where we pick a sublattice with $n = 1$. These two states, corresponding to the two sublattices, maximize the number of occupied sites, and thus $\mu \sum n$, while avoiding any occupied nearest neighbors. The two checkerboard states spontaneously break translation symmetry and are transformed into each other if we shift by one lattice site. This is a solid phase. By contrast, as $T \rightarrow \infty$, the ensemble (3) is uniform: $P(\mathbf{n}) = 2^{-L^2}$. Here L is the number of vertices along a side of the square. This ensemble is disordered: all configurations are equally likely. In fact, this last statement is true at $T = \infty$ ($\beta = 0$) independently of H , since all \mathbf{n} are valid configurations. This is the heart of a no-go theorem^{30,31} on entropic order as $T \rightarrow \infty$ (see SM). Indeed, many familiar systems observed in nature are disordered at high T .

For μ outside the range $[0, 4U]$, the model has no phase transitions and the zero-temperature ground state is unique; all sites either have $n = 0$ (if $\mu < 0$) or $n = 1$ (if $\mu > 4U$).

Results

We are going to explore how the no-go theorem above can be avoided. Clearly, this is only possible if the thermal distribution (3) does not

look uniform as $\beta \rightarrow 0$. On the $L \times L$ square lattice, one way to achieve this is if there are an infinite number of microstates: e.g., $n_v \in \{0, 1, 2, \dots\}$ can take any non-negative integer value. Just as there is not a uniform distribution over the integers, a uniform $\beta = 0$ ensemble will then not exist. We choose

$$H = U \sum_{u \sim v} n_u^2 n_v^2 + \sum_v n_v. \quad (6)$$

Note the similarity with (5) where we have fixed $\mu = -1$; indeed, we are choosing to measure energy scales (T, U) relative to $|\mu|$. Our model (6) is well defined; it has finitely many states \mathbf{n} obeying $H(\mathbf{n}) \leq E$ for any finite E . The repulsion U between particles at adjacent sites can grow slower than quadratically (but faster than linearly) in the n_u , without changing the conclusions.

Intuitively, as $\beta \rightarrow \infty$, the dominant states in the thermal ensemble will have $n_v = 0$ on most sites, since each particle costs energy. For a large but finite $\beta \gg 1$, some finite fraction $\sim e^{-\beta}$ of sites will be occupied, most with a single particle. Since this fraction of sites is small, the occupied sites can essentially be drawn randomly, so there is no long-range order. This is a gas phase.

We now claim that for sufficiently small $\beta < \beta_c$, the model is an entropic ordered solid. To justify this claim, notice that if one site is occupied but none of its neighbors are, the typical number of particles \bar{n}_1 obeys $\beta \bar{n}_1 \sim 1$, or $\bar{n}_1 \sim T$. In contrast, if two adjacent sites both have \bar{n}_2 particles, $\beta \bar{n}_2^4 \sim 1$ or $\bar{n}_2 \sim T^{1/4}$. If we consider the checkerboard arrangement from before, we can occupy half of the sites leading to partition function $\bar{n}_1^{L^2/2} \sim T^{L^2/2}$, which is much larger than $\bar{n}_2^{L^2} \sim T^{L^2/4}$ if we consider the disordered state. This suggests that the dominant contribution to $Z(\beta)$ comes from checkerboard-like states for sufficiently small β . Therefore the high-temperature phase is a solid phase that spontaneously breaks the lattice translational symmetry.

An analytic formula for $Z(\beta)$ is not known to us, but we can deduce the phase diagram by numerical Markov Chain simulations^{32,33}, using a classical Gibbs sampler to (approximately) sample microstates \mathbf{n} with probability (3). The results are summarized in Fig. 1a, where typical states clearly are disordered at low temperature and ordered at high temperature, with the order manifesting in the anticipated checkerboard pattern. In statistical physics, we can more quantitatively diagnose the presence of order by calculating the order parameter

$$\Delta = \frac{1}{L^4} \left\langle \left(\sum_{x,y=1}^L (-1)^{x+y} n_{(x,y)} \right)^2 \right\rangle = \frac{\langle (N_A - N_B)^2 \rangle}{L^4}. \quad (7)$$

which counts the imbalance in total particles occupying the two possible checkerboards, parameterized by whether $x + y$ is an even (A sublattice) or odd (B sublattice) integer. The factor L^{-4} in front ensures that $\Delta > 0$ as $L \rightarrow \infty$ in a solid phase, while $\Delta = 0$ as $L \rightarrow \infty$ in a disordered phase. Figure 1b demonstrates that Δ takes an L -independent value for $\beta \lesssim \beta_c \approx 0.19$ at $U = 1$, suggesting that $\beta_c \approx 0.19$ is the critical temperature separating order and disorder. We expect that the universality class of this transition matches the two-dimensional Ising model, which we confirm by a standard scaling analysis in Fig. 1c (see SM for details).

An interesting limit that we can say more about is to take $U \rightarrow \infty$ with fixed β . This is a variant of the hardcore lattice gas, which is typically defined as follows: letting $n_u \in \{0, 1\}$ ^{34,35}, we wish to restrict the configuration space only to configurations where $n_u n_v = 0$ for any pair

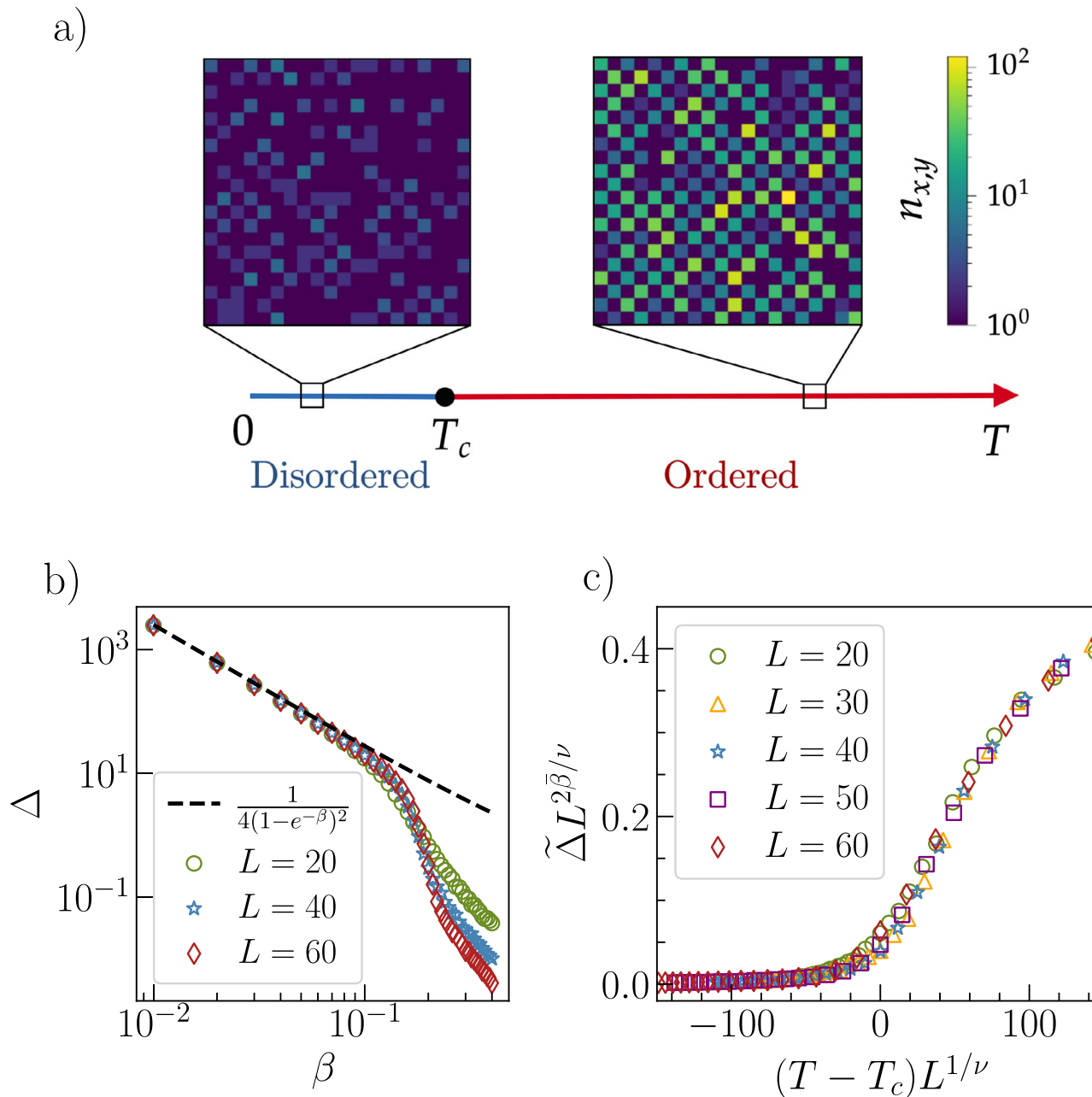


Fig. 1 | Phase diagram and finite-size scaling of the classical bosonic lattice gas.

a The phase diagram of the classical bosonic lattice gas (6). We choose two points $T=1/\beta=2$ and $T=20$ and show the corresponding late-time snapshots of the model on a 20×20 square lattice simulated using the Monte Carlo algorithm. The color on each site denotes the number of particles on a site, with brighter color representing more particles. **b** The square of the particle density difference of sublattices A and B

vs β for different system sizes on a log-log scale. The black dashed line corresponds to the theoretical prediction assuming a defect-free solid. **c** A finite-size scaling analysis of the order parameter $\tilde{\Delta}$, defined analogously to Δ but with $n_{(x,y)}$ replaced by $1 - \delta_{n_{(x,y)}, 0}$, is consistent with the Ising universality class. For all simulations, we take the interaction strength $U = 1$, which gives the critical point $T_c = 1/\beta_c \approx 1/0.19$.

of adjacent sites $u \sim v$. Then we find

$$Z = \sum_{\{n_u\} \text{ with } n_u n_v = 0 \text{ if } u \sim v} z^{\sum_u n_u} = \sum_{M=0}^{L^2/2} F_M z^M \quad (8)$$

where $z = e^{\beta\mu}$. Notice that $\frac{L^2}{2}$ is the maximal number of occupied sites. We have defined F_M as the number of ways to occupy M sites on the $L \times L$ lattice obeying the constraint. The model (8) is the $U \rightarrow \infty$ limit of the model (5).

If $\mu > 0$, then the low temperature phase ($z \rightarrow \infty$) is a solid and the high temperature phase ($z \rightarrow 1$) is a gas. If $\mu < 0$, there is a gas at all

temperatures. The phase transition at $\mu > 0$ on the square lattice is in the Ising universality class and occurs at $z \approx 3.79^{34,36}$.

Now we return to the $U \rightarrow \infty$ limit of our model (6). Because we are no longer restricted to having 0 or 1 particles per site, we now find

$$Z(\beta) = \sum_{M=0}^{N^2/2} F_M (e^{-\beta} + e^{-2\beta} + \dots)^M = \sum_{M=0}^{N^2/2} \frac{F_M}{(e^\beta - 1)^M}. \quad (9)$$

We see that the phase diagram is exactly flipped relative to the standard hardcore lattice gas: now $z = (e^\beta - 1)^{-1}$ is small at low temperature ($\beta \rightarrow \infty$), and large at high temperature ($\beta \rightarrow 0$). Therefore, the model

describes a low-temperature gas and a high-temperature entropically ordered solid.

The mechanism underlying the formation of this high-temperature solid is that sacrificing the mobility of the particles and placing them in a checkerboard pattern allows to gain entropy due to the fluctuations on site. In fact, it is not necessary to allow an arbitrary number of particles at each site for this mechanism to work! If we denote the maximum allowed number of particles at each site by K , so long as $K \geq 4$, we still find a solid at high temperature on the rectangular lattice.

This model with finite K (and $U = \infty$) has finitely many states, but still leads to high temperature order, because the configuration space is not a direct product, due to the hardcore constraint. Similarly, one can construct other examples of high-temperature order in systems at a fixed charge sector. For example, the model (8) at a fixed density will have high-temperature order for sufficiently large density (that corresponds to fixed $\beta\mu$ with $\beta \rightarrow 0$). We focus on realizing entropic order without such constraints.

Lastly, we note that there are infinitely many terms (such as $\epsilon \sum_v n_v^k$ for any $k > 2$) that one could add to (6) that change the phase diagram as $T \rightarrow \infty$. In this case, the entropic order will persist below a critical temperature T_c , which diverges as $\epsilon \rightarrow 0$.

To illustrate that (6) is just one of many simple models with entropic order, we now describe some exactly solvable models, starting with a classical model of ferromagnetism at high T , based on the Ising model. Let $s_v \in \{\pm 1\}$ be spins sitting on the vertices of a square lattice, while $n_{uv} \in \{0, 1, 2, \dots\}$ are bosons sitting on the edges; take

$$H = \sum_{u \sim v} (a - b s_u s_v) (n_{uv} + 1) \quad (10)$$

where $a > b > 0$. This model has a twofold degenerate ground state with $s_u = 1$ or $s_u = -1$. The model therefore has the usual magnetic order at low temperatures.

We now evaluate the partition function by exactly summing over n_{uv} , and find

$$Z(\beta) = \sum_{s_v} \sum_{n_{uv}} e^{-\beta H} = \sum_{s_u = \pm 1} e^{-A + B s_u s_v} \quad (11)$$

where we define

$$e^{-2A} = \frac{e^{-2\beta a}}{(1 - e^{-\beta(a+b)})(1 - e^{-\beta(a-b)})}, \quad (12a)$$

$$e^{2B} = e^{2\beta b} \frac{1 - e^{-\beta(a+b)}}{1 - e^{-\beta(a-b)}}. \quad (12b)$$

Equation (11) takes the form of an Ising partition function at effective inverse temperature $B(\beta)$. At $\beta \rightarrow \infty$, $B \rightarrow \infty$ and the model is in the ordered phase, as anticipated. At $\beta \rightarrow 0^+$, we have that $B(0) = \frac{1}{2} \log \frac{a+b}{a-b}$. Using the exact critical temperature of the Ising model on the square lattice, we conclude that if $\frac{a}{b} < 1 + \sqrt{2}$, the system (10) has ferromagnetism (long-range order in s) at all temperatures. Indeed, one can check that B is a monotonically decreasing function of temperature, so one never leaves the magnetically ordered phase. The high temperature magnetism arises from entropic order; when the discrete spins form a ferromagnet, they enable vastly more fluctuations in the number of bosons n_{uv} . The reduction in entropy from the spins is outweighed by the gain in entropy from n_{uv} fluctuations. If one is only interested in obtaining very high temperature ordered phases, it is not necessary to have infinitely many bosons $n_{uv} \in \{0, 1, 2, \dots\}$: limiting $n_{uv} \leq K$ is sufficient. The same comments apply for the constructions below.

It is possible to use similar link bosons n_{uv} to construct ordered high temperature phases in a broad variety of other models. For example, adding link bosons to a three-dimensional classical XY model, we can obtain superfluidity at arbitrarily high temperatures. Similarly, adding bosons to the four-dimensional toric code³⁷, we can construct examples of entropic topologically ordered states at high temperature. This construction demonstrates a clear loophole in the recent theorem that all quantum lattice models have no quantum entanglement at sufficiently high T ¹⁰. As in the classical setting, this theorem assumed that the local Hilbert space was finite-dimensional, an assumption violated by the bosons above. Details can be found in the SM.

Models of entropic order also exist in continuous space, i.e., in QFTs as first considered in ref. 38. To be able to push entropic order all the way to infinite temperature in QFT, the QFT has to be UV-complete, i.e., exist independently of an underlying lattice model. Our goal here is to show that the QFTs of refs. 11,12,21 are entropically ordered at high temperature: ordered states carry more entropy than the disordered ones.

For simplicity, we will focus on QFTs in $2 < d < 3$ spatial dimensions (see SM for details). A similar, albeit more complicated, analysis can be carried out in $d = 2$ as well (the conclusions remain the same).

The model that we study contains a boson ψ and a vector of N bosons ϕ with Lagrangian (in Euclidean signature)

$$\mathcal{L} = \frac{1}{2} (\partial\psi)^2 + \frac{1}{2} (\partial\phi)^2 + \frac{\lambda}{4N} (\phi^2 - \psi^2)^2, \quad (13)$$

This model has local interactions, and the energy is bounded from below. The classical Hamiltonian has a degeneracy of ground states with $\phi^2 = \psi^2$ but this degeneracy is lifted quantum mechanically^{11,12,21}, and there is a unique ground state at zero temperature in the full theory. In fact, the model (13) leads to an interacting conformal theory at zero temperature. That conformal theory is multi-critical since several relevant parameters are tuned to zero. We investigate the high temperature behavior of the multi-critical fixed point, since that fixes the high temperature behavior of the nearby ordered and disordered zero temperature phases as well.

Our goal is to calculate the free energy of a configuration with average field configurations $\bar{\phi} = (\bar{\phi}_1, 0, \dots, 0)$ and $\bar{\psi}$. Using standard techniques of thermal field theory, in the large N limit, the answer is given by

$$\frac{\mathcal{F}}{N} \approx -c_1 T^{d+1} + c_2 T^{-\frac{2}{d-2}} \left(c_3 T^{d-1} + \phi^2 - \psi^2 \right)^{\frac{d}{d-2}} + \dots \quad (14)$$

where $c_{1,2,3} > 0$ are constants and \dots stand for terms which are sub-leading at large N . \mathcal{F} above still has a manifold of thermal minima $c_3 T^{d-1} + \phi^2 - \psi^2 = 0$. This degeneracy is resolved once one includes further corrections in the $1/N$ expansion. The final answer is that^{11,12,21} \mathcal{F} is minimized when $\phi^2 = 0$ and $\psi^2 = c_3 T^{d-1}$. Since $\psi^2 > 0$, the \mathbb{Z}_2 symmetry $\psi \rightarrow -\psi$ of (13) is spontaneously broken at any $T > 0$. To see that this ordered state maximizes the entropy density, we calculate it explicitly: at $\bar{\phi} = 0$,

$$\frac{S}{N} = -\frac{1}{N} \left(\frac{\partial \mathcal{F}}{\partial T} \right)_{\phi, \psi} = (d+1)c_1 T^d - \frac{T^{-\frac{d}{d-2}} c_2 (c_3 T^{d-1} - \bar{\psi}^2)^{\frac{2}{d-2}}}{d-2} (2\bar{\psi}^2 + (d^2 - d - 2)c_3 T^{d-1}). \quad (15)$$

Indeed, ordering $\bar{\psi}$ increases the overall entropy.

Entropic order as $T \rightarrow \infty$ persists when the theory is deformed by relevant perturbations. For example, adding $\epsilon\psi^2$ to (13) simply causes

the same perturbation to (14); at large T , the minimum of \mathcal{F} remains at $\bar{\psi} \neq 0$. If irrelevant perturbations are added, the theory is not UV-complete and therefore the question of high-temperature order is not meaningful within the framework of QFT.

Now that we understand how to build quantum field theories and lattice models with entropic order, we discuss a model of high-temperature superconductivity. The standard Bardeen–Cooper–Schrieffer (BCS) model for superconductivity³⁹ contains a finite density Fermi surface of spin- $\frac{1}{2}$ electrons $\psi_{\uparrow,\downarrow}$ with an attractive two-body interaction, leading to a spontaneously broken U(1) symmetry, measured by a non-vanishing order parameter $\Delta = \langle \psi_{\uparrow} \psi_{\downarrow} \rangle$. At low temperatures relative to a cutoff energy ω_* , which can be large compared to room temperature, we find superconductivity whenever the BCS gap equation (see SM) has a solution:

$$\frac{1}{g_{\text{eff}}} = \nu \int_0^{\beta\omega_*} dx \frac{\tanh\left(\frac{1}{2}\sqrt{x^2 + (\beta\Delta)^2}\right)}{\sqrt{x^2 + (\beta\Delta)^2}}, \quad (16)$$

where ν is the fermionic density of states, and g_{eff} is the effective interaction strength. Regardless of the value of Δ , the integral above goes to zero as $\beta \rightarrow 0$. Therefore, at sufficiently high temperature, one finds no solution if g_{eff} is temperature independent, and thus there is no superconductivity at high temperature. Crucially, we can build a model where $g_{\text{eff}}(T)$ increases with temperature. Keeping details in the SM, we write a theory of $N \gg 1$ critical bosons coupled to $N \gg 1$ spin- $\frac{1}{2}$ fermions, similar to (13), but where ψ^2 is replaced by $|\Delta|^2$. We find entropic order, which manifests in a g_{eff} which grows at higher temperature. This temperature dependence of g_{eff} enables superconductivity for all $\beta\omega_* \geq 1$ (the effective field theory does not make sense at higher temperatures). This is in contrast to the usual case, where superconductivity persists up to $\beta_c \sim \omega_*^{-1} e^{1/g_{\text{eff}}\nu} \gg \omega_*^{-1}$, i.e., we have found an exponential increase in T_c .

Discussion

We have described entropic order, whereby typical high-energy states, of either classical or quantum systems, can exhibit long-range order and/or quantum entanglement. This counterintuitive idea is possible because sometimes ordering a subset of degrees of freedom enables many more possible microstates for the rest.

We have demonstrated this concept for lattice gases that turn into solids at high T , magnets that remain magnetic at high T , persistent superfluidity, topological order, and high- T_c superconductivity. Entropic order was also seen to explain the recent demonstration of $T \rightarrow \infty$ order in QFT.

An important ingredient in our construction of high-temperature superconductivity was interacting bosons, which, under the circumstances we described, lead to entropically driven superconductivity. This is in contrast to simply enhancing the effective zero-temperature coupling⁴⁰. It would be very interesting if such ideas were realizable.

Data availability

The numerical data generated in this study are provided in Supplementary Data 2.

Code availability

The code used in this study are provided in Supplementary Data 1.

References

1. Kao, K. C. *Dielectric Phenomena in Solids* (Elsevier, 2004).
2. Plazanet, M., Floare, C., Johnson, M. R., Schweins, R. & Trommsdorff, H. P. Freezing on heating of liquid solutions. *J. Chem. Phys.* **121**, 5031 (2004).
3. Radzihovsky, L., Frey, E. & Nelson, D. R. Novel phases and reentrant melting of two-dimensional colloidal crystals. *Phys. Rev. E* **63**, 031503 (2001).
4. Sprakler, J., Zacccone, A., Spaepen, F., Schall, P. & Weitz, D. A. Direct observation of entropic stabilization of bcc crystals near melting. *Phys. Rev. Lett.* **118**, 088003 (2017).
5. Schupper, N. & Shnerb, N. M. Spin model for inverse melting and inverse glass transition. *Phys. Rev. Lett.* **93**, 037202 (2004).
6. Pomeranchuk, I. On the theory of liquid He-3. *J. Exp. Theor. Phys.* **20**, 919 (1950).
7. Rozen, A. et al. Entropic evidence for a Pomeranchuk effect in magic-angle graphene. *Nature* **592**, 214–219 (2021).
8. Villain, J., Bidaux, R., Carton, J.-P. & Conte, R. Order as an effect of disorder. *J. Phys.* **41**, 1263 (1980).
9. Kliesch, M., Gogolin, C., Kastoryano, M. J., Riera, A. & Eisert, J. Locality of temperature. *Phys. Rev. X* **4**, 031019 (2014).
10. Bakshi, A., Liu, A., Moitra, A. & Tang, E. High-Temperature Gibbs States are Unentangled and Efficiently Preparable. *2024 IEEE 65th Annual Symposium on Foundations of Computer Science (FOCS)*, 1027–1036 (Chicago, IL, USA, 2024). <https://doi.org/10.1109/FOCS61266.2024.00068>.
11. Chai, N. et al. Symmetry breaking at all temperatures. *Phys. Rev. Lett.* **125**, 131603 (2020).
12. Chai, N. et al. Thermal order in conformal theories. *Phys. Rev. D* **102**, 065014 (2020).
13. Liendo, P., Rong, J. & Zhang, H. Spontaneous breaking of finite group symmetries at all temperatures. *SciPost Phys.* **14**, 168 (2023).
14. Chai, N., Rabinovici, E., Sinha, R. & Smolkin, M. The bi-conical vector model at 1/N. *J. High Energy Phys.* **05**, 192 (2021).
15. Chaudhuri, S., Choi, C. & Rabinovici, E. Thermal order in large N conformal gauge theories. *J. High Energy Phys.* **04**, 203 (2021).
16. Bajc, B., Lugo, A. & Sannino, F. Asymptotically free and safe fate of symmetry nonrestoration. *Phys. Rev. D* **103**, 096014 (2021).
17. Nakayama, Y. On the trace anomaly of the Chaudhuri–Choi–Rabinovici model. *Symmetry* **13**, 276 (2021).
18. Chaudhuri, S. & Rabinovici, E. Symmetry breaking at high temperatures in large N gauge theories. *J. High Energy Phys.* **08**, 148 (2021).
19. Agrawal, P. & Nee, M. Avoided deconfinement in Randall–Sundrum models. *J. High Energy Phys.* **10**, 105 (2021).
20. Hawashin, B., Rong, J. & Scherer, M. M. UV complete local field theory of persistent symmetry breaking in 2+1 dimensions. *Phys. Rev. Lett.* **134**, 041602 (2025).
21. Komargodski, Z. & Popov, F. K. Temperature-resistant order in 2+1 dimensions. *Phys. Rev. Lett.* **135**, 091602 (2025).
22. Buchel, A. Fate of the conformal order. *Phys. Rev. D* **103**, 026008 (2021).
23. Buchel, A. Thermal order in holographic CFTs and no-hair theorem violation in black branes. *Nucl. Phys. B* **967**, 115425 (2021).
24. Buchel, A. Compactified holographic conformal order. *Nucl. Phys. B* **973**, 115605 (2021).
25. Buchel, A. The quest for a conifold conformal order. *J. High Energy Phys.* **08**, 080 (2022).
26. Buchel, A. Holographic conformal order with higher derivatives. *Nucl. Phys. B* **1004**, 116578 (2024).
27. Chai, N., Dymarsky, A., Goykhman, M., Sinha, R. & Smolkin, M. A model of persistent breaking of continuous symmetry. *SciPost Phys.* **12**, 181 (2022).
28. Chai, N., Dymarsky, A. & Smolkin, M. Model of persistent breaking of discrete symmetry. *Phys. Rev. Lett.* **128**, 011601 (2022).
29. Lee, T. D. & Yang, C. N. Statistical theory of equations of state and phase transitions. II. Lattice gas and Ising model. *Phys. Rev.* **87**, 410–419 (1952).
30. Dobrushin, R. L. Prescribing a system of random variables by the help of conditional distributions. *Theor. Prob. Appl.* **15**, 469 (1970).

31. Simon, B. *The Statistical Mechanics of Lattice Gases*, Vol. I (Princeton Univ. Press, 1993).
32. Metropolis, N., Rosenbluth, A. W., Rosenbluth, M. N., Teller, A. H. & Teller, E. Equation of state calculations by fast computing machines. *J. Chem. Phys.* **21**, 1087–1092 (1953).
33. Hastings, W. K. Monte Carlo sampling methods using Markov chains and their applications. *Biometrika* **57**, 97–109 (1970).
34. Baxter, R. J., Enting, I. G. & Tsang, S. K. Hard-square lattice gas. *J. Stat. Phys.* **22**, 465–489 (1980).
35. Baxter, R. J. *Exactly Solved Models in Statistical Mechanics* (Academic Press, 1982).
36. Fernandes, H. C. M., Arenzon, J. J. & Levin, Y. Monte Carlo simulations of two-dimensional hard core lattice gases. *J. Chem. Phys.* **126**, 114508 (2007).
37. Alicki, R., Horodecki, M., Horodecki, P. & Horodecki, R. On thermal stability of topological qubit in Kitaev's 4D model. *Open Syst. Inf. Dyn.* **17**, 1–20 (2010).
38. Weinberg, S. Gauge and global symmetries at high temperature. *Phys. Rev. D* **9**, 3357–3378 (1974).
39. Bardeen, J., Cooper, L. N. & Schrieffer, J. R. Theory of superconductivity. *Phys. Rev.* **108**, 1175–1204 (1957).
40. Lederer, S., Schattner, Y., Berg, E. & Kivelson, S. A. Enhancement of superconductivity near a nematic quantum critical point. *Phys. Rev. Lett.* **114**, 097001 (2015).

Acknowledgements

We thank Sarang Gopalakrishnan, David Huse, and Leo Radzihovsky for interesting discussions. This work was supported by the National Science Foundation under CAREER Grant DMR-2145544 (X.H., A.L.) and Grant PHY-2310283 (Z.K.), by the Air Force Office of Scientific Research under Grant FA9550-24-1-0120 (Y.H., A.L.), and by the US-Israel Binational Science Foundation under Grant 2018204 (Z.K.).

Author contributions

Y.H. performed numerical simulations and analyzed data. X.H., Z.K., A.L., and F.K.P. performed analytical calculations. All authors contributed to writing the manuscript and developing the project.

Competing interests

The authors declare no competing interests.

Additional information

Supplementary information The online version contains supplementary material available at <https://doi.org/10.1038/s41467-025-66797-3>.

Correspondence and requests for materials should be addressed to Andrew Lucas.

Peer review information *Nature Communications* thanks the anonymous reviewers for their contribution to the peer review of this work.

Reprints and permissions information is available at <http://www.nature.com/reprints>

Publisher's note Springer Nature remains neutral with regard to jurisdictional claims in published maps and institutional affiliations.

Open Access This article is licensed under a Creative Commons Attribution-NonCommercial-NoDerivatives 4.0 International License, which permits any non-commercial use, sharing, distribution and reproduction in any medium or format, as long as you give appropriate credit to the original author(s) and the source, provide a link to the Creative Commons licence, and indicate if you modified the licensed material. You do not have permission under this licence to share adapted material derived from this article or parts of it. The images or other third party material in this article are included in the article's Creative Commons licence, unless indicated otherwise in a credit line to the material. If material is not included in the article's Creative Commons licence and your intended use is not permitted by statutory regulation or exceeds the permitted use, you will need to obtain permission directly from the copyright holder. To view a copy of this licence, visit <http://creativecommons.org/licenses/by-nc-nd/4.0/>.

© The Author(s) 2025